

COMPARATIVE STUDY OF ELECTROCHEMICAL  
TRANSDUCER FABRICATION METHODS WITH  
GLUCOSE OXIDASE AS RECOGNITION LAYER

BY

NURUL IZZATI BINTI RAMLI

A thesis submitted in fulfilment of the requirement for the  
degree of Master of Science (Biotechnology Engineering)

Kulliyyah of Engineering  
International Islamic University Malaysia

NOVEMBER 2020

## ABSTRACT

Combination of reduced graphene oxide (rGO) with a conductive polymer, poly(3,4-ethylenedioxythiophene):poly(styrene sulfonate) (PEDOT:PSS) is promising as transducer material for electrochemical biosensors. However, fundamental research into this composite behaviour is essential for generating the necessary scientific understanding to realize a non-invasive glucose monitoring approach. In this study, the rGO-PEDOT:PSS modified electrodes were fabricated with four different methods (method A, B, C, and D) where the fabrication parameters such as reduction cycles, sequence and glucose oxidase immobilisation techniques were varied. The aim is to elucidate how these fabrication parameters can affect the electrochemical reversibility, mass transport properties, heterogeneous electron transfer rate constant ( $k^0$ ) and effective surface area ( $A_{\text{eff}}$ ) of rGO-PEDOT:PSS materials in which can be determined from cyclic voltammetry (CV). This study also utilized machine learning algorithm to model the data from CV results where the most accurate model was used to analyse the interaction strength between the input and output data. From the electrochemical analysis, the ferri/ferrocyanide redox couple  $[\text{Fe}(\text{CN})_6]^{3-/4-}$  shows quasi-reversible and diffusion-controlled behaviour on rGO-PEDOT:PSS-modified SPCEs of all fabrication method. In terms of  $k^0$ , each fabrication methods generated different trend of  $k^0$  value with increasing reduction cycles. Overall, the range of  $k^0$  for rGO-PEDOT:PSS-modified SPCE are from  $0.52 \times 10^{-5}$  to  $4 \times 10^{-5}$  cm/s. We also found that the highest  $A_{\text{eff}}$  value with respect to fabrication method were obtained from different number of reduction cycles. Fabrication method A gave the highest  $A_{\text{eff}}$  when the composite was reduced for 5 reduction cycles ( $16.41 \text{ cm}^2$ ). For methods B and D, the highest  $A_{\text{eff}}$  obtained was for 30 reduction cycles ( $17.48 \text{ cm}^2$  for method B and  $6.43 \text{ cm}^2$  for method D) while for method C, the highest  $A_{\text{eff}}$  value was obtained for 15 reduction cycles ( $21.41 \text{ cm}^2$ ). For SVM analysis, data from CV ( $\Delta E_p$  and  $I_{pc}$ ) and the fabrication parameters were used to construct a prediction model. Linear and non-linear kernels were compared, and the best performance was showed by radial basis function (RBF) kernel with a perfect accuracy of 100%. The RBF kernel was then used to measure the interaction between input and output variables in which the kernel model demonstrated the strongest interaction between reduction cycles and  $\Delta E_p$ . In conclusion, this study reveals the effect of fabrication parameters on electrochemical characteristics of rGO-PEDOT:PSS-modified SPCEs and the capability of machine learning algorithm to model data and provide deeper insights on the fabrication process, opening a new route for development of non-invasive glucose biosensors.

## خلاصة البحث

يُعد مركب أكسيد الجرافين المختزل (rGO) مع البوليمر الموصل بولي (٤، ٣-إيثيلين ديوكسي ثيوفين): بولي (ستايرين سلفونات) (PEDOT: PSS) أحد المركبات الواعدة لكونها مادة محمولة لأجهزة الاستشعار الحيوية الكهروكيميائية. ومع ذلك، فإن البحث الأساسي في سلوك هذا المركب ضروري لتوليد الفهم العلمي المطلوب لتحقيق نهج غير غازي لمراقبة الجلوكوز. تم تصنيع أقطاب rGO-PEDOT: PSS المعدلة في هذه الدراسة بأربع طرق مختلفة (الطريقة A و B و C و D) حيث اختلفت معاملات التصنيع مثل دورات الاختزال والتسلسل وتقنيات تثبيت أو أكسيدات الجلوكوز. والهدف يكمن في توضيح كيفية تأثير عوامل التصنيع على ثابت معدل التفاعل ( $k^0$ ) ومنطقة السطح الفعالة ( $A_{eff}$ ) الخاص بمواد rGO-PEDOT:PSS التي يمكن تحديدها من المقياس الفولطي الدوري (CV). استخدمت هذه الدراسة أيضًا خوارزمية التعلم الآلي لنمذجة بيانات نتائج المقياس الفولطي الدوري حيث تم استخدام النموذج الأكثر دقة لتحليل قوة التفاعل بين بيانات الإدخال والإخراج. وبالنظر إلى التحليل الكهروكيميائي، يُظهر زوجا الأكسدة والاختزال فيري / فيروسيانيد  $[Fe(CN)_6]^{3-/4-}$  سلوك شبه قابل للعكس والتحكم في الانتشار على rGO-PEDOT: PSS المعدلة من SPCE لجميع طرق التصنيع. أما من حيث  $k^0$ ، فكل طرق التصنيع أنتجت اتجاهات مختلفًا لقيمة  $k^0$  مع زيادة دورات الإرجاع. بشكل عام، يتراوح نطاق  $k^0$  لـ rGO-PEDOT:PSS المعدل ما بين  $0.52 \times 10^{-5}$  إلى  $4 \times 10^{-5}$  سم في الثانية. وقد وجدنا أيضًا أنه تم الحصول على أعلى قيمة لـ  $A_{eff}$  فيما يتعلق بطريقة التصنيع من عدد مختلف من دورات الاختزال. أعطت طريقة التصنيع A أعلى نسبة  $A_{eff}$  عندما تم تخفيض المركب إلى ٥ دورات إرجاع (١٦،٤١ سم<sup>٢</sup>). أما بالنسبة للطريقتين B و D، فإن أعلى  $A_{eff}$  تم الحصول عليه مع ٣٠ دورة إرجاع (١٧،٤٨ سم<sup>٢</sup> للطريقة B و ٦،٤٣ سم<sup>٢</sup> للطريقة D) بينما بالنسبة للطريقة C، فتم الحصول على أعلى قيمة  $A_{eff}$  مع ١٥ دورة إرجاع (٢١،٤١ سم<sup>٢</sup>). بالنسبة لتحليل شعاع الدعم الآلي، تم استخدام بيانات المقياس الفولطي الدوري ( $\Delta E_p$  and  $I_{pc}$ ) وعوامل التصنيع لبناء نموذج تنبؤ. تمت مقارنة النوى الخطية وغير الخطية، وأظهرت نواة وظيفة الأساس الشعاعي (RBF) أفضل أداء بدقة مثالية بنسبة ١٠٠٪. ثم تم استخدام نواة RBF لقياس التفاعل بين متغيرات المدخلات والمخرجات حيث أظهر نموذج النواة أقوى تفاعل بين دورات الاختزال و  $\Delta E_p$ . وفي النهاية، تكشف هذه الدراسة عن تأثير عوامل التصنيع على الخصائص الكهروكيميائية لـ rGO-PEDOT: PSS المعدلة SPCEs، وقدرة خوارزمية التعلم الآلي على نمذجة البيانات وتقديم رؤى أعمق حول عملية التصنيع، وفتح طريق جديد لتطوير أجهزة الاستشعار الحيوية للجلوكوز غير الغازية.

## APPROVAL PAGE

I certify that I have supervised and read this study and that in my opinion, it conforms to acceptable standards of scholarly presentation and is fully adequate, in scope and quality, as a thesis for the degree of Master of Science (Biotechnology Engineering).

.....  
Wan Wardatul Amani Wan Salim  
Supervisor

.....  
Mohd Firdaus Abd-Wahab.  
Co-Supervisor

I certify that I have read this study and that in my opinion it conforms to acceptable standards of scholarly presentation and is fully adequate, in scope and quality, as a thesis for the degree of Master of Science (Biotechnology Engineering).

.....  
Izzat Fahimuddin Mohamed  
Suffian  
Internal Examiner

.....  
Lee Hooi Ling  
External Examiner

This thesis was submitted to the Department of Biotechnology Engineering and is accepted as a fulfilment of the requirement for the degree of Master of Science (Biotechnology Engineering).

.....  
Nor Fadhillah Mohamed Azmin  
Head, Department of  
Biotechnology Engineering

This thesis was submitted to the Kulliyyah of Engineering and is accepted as a fulfilment of the requirement for the degree of Master of Science (Biotechnology Engineering).

.....  
Sany Izan Ihsan  
Dean, Kulliyyah of Engineering

## DECLARATION

I hereby declare that this thesis is the result of my own investigations, except where otherwise stated. I also declare that it has not been previously or concurrently submitted as a whole for any other degrees at IIUM or other institutions.

Nurul Izzati binti Ramli

Signature .....

Date .....

**INTERNATIONAL ISLAMIC UNIVERSITY MALAYSIA**

**DECLARATION OF COPYRIGHT AND AFFIRMATION OF  
FAIR USE OF UNPUBLISHED RESEARCH**

**COMPARATIVE STUDY OF ELECTROCHEMICAL  
TRANSDUCER FABRICATION METHODS WITH GLUCOSE  
OXIDASE AS RECOGNITION LAYER**

I declare that the copyright holders of this thesis are jointly owned by the student and IIUM.

Copyright © 2020 Nurul Izzati binti Ramli and International Islamic University Malaysia. All rights reserved.

No part of this unpublished research may be reproduced, stored in a retrieval system, or transmitted, in any form or by any means, electronic, mechanical, photocopying, recording or otherwise without prior written permission of the copyright holder except as provided below

١. Any material contained in or derived from this unpublished research may be used by others in their writing with due acknowledgement.
٢. IIUM or its library will have the right to make and transmit copies (print or electronic) for institutional and academic purposes.
٣. The IIUM library will have the right to make, store in a retrieved system and supply copies of this unpublished research if requested by other universities and research libraries.

By signing this form, I acknowledged that I have read and understand the IIUM Intellectual Property Right and Commercialization policy.

Affirmed by Nurul Izzati binti Ramli

.....  
Signature

.....  
Date

## ACKNOWLEDGEMENTS

Firstly, I wish to dedicate this work to my dear parents and family. Thank you for the continuous and unwavering support, love and encouragement throughout this period of study. Thank you for sharing all the hard times with me and always being with me in every step I take in life.

I would like to express my sincerest gratitude to my supervisor, Dr. Wan Wardatul Amani Wan Salim for her invaluable encouragement, motivation, and constructive comments throughout all stages of this research. Without her guidance and patience, this research would not have reached its final form. I am beyond grateful for the opportunity to work with her since my undergraduate years and for all unforgettable experiences and working exposure that I got for being one of her students.

I also wish to express my appreciation and gratitude to my co-supervisor, Dr. Mohd. Firdaus Abd-Wahab, whom I admire most for his vast knowledge. Thank you for the continuous support, time, effort, and brilliant insights for this project.

To my ARG colleague, Sr. Alya Batrisya Ismail, thank you for all the advice, encouragement and support, and for taking care of me as her own sister. To my other ARG colleagues, Sr. Habibah Farhana, Br. Benoudjit Abdel Mohsen and Sr. Nasteho Ali, thank you for sharing with me your knowledge and skills. For Br. Iwan Syafie, thank you for helping me out with my project. To other ARG colleagues, fellow FYP students and interns, thank you for the support and kindness.

A special thanks to my viva examiners, Dr. Izzat Fahimuddin Mohamed Suffian and Dr. Lee Hooi Ling for their thoughtful suggestions and comments that allow me to improve my thesis. Not to forget, Dr. Afidalina Tumian, Dr. Ricca Rahman Nasaruddin and Dr. Wan Mohd. Fazli Wan Nawawi for their constructive feedbacks and advice during Comprehensive Exam (CE) and research progress presentation.

Last but not least, thank you for my dearest friends, especially Aina Aqilah M. Hanafiah, Sarah Amalina Adli, Ain Nadhirah Bahari, Ainul Farhani Ahmad Nizam, Ummul Madihah Mohd Rashidi, Norazilah Mohamed Paid, and Amira Husna Ramdzan, for being part of my support system.

# TABLE OF CONTENTS

Abstract .....	iii
Abstract in Arabic .....	iv
Approval Page.....	v
Declaration .....	vi
Copyright Page.....	vii
Acknowledgements.....	viii
Table of Contents .....	ix
List of Tables .....	xii
List of Figures .....	xiii
List of Abbreviations .....	xix
List of Symbols .....	xx
<b>CHAPTER ONE: INTRODUCTION .....</b>	<b>1</b>
1.1 Background of the Study .....	1
1.2 Problem Statement.....	5
1.3 Research Objectives.....	6
1.4 Research Scope .....	6
1.5 Thesis Organization .....	7
<b>CHAPTER TWO: LITERATURE REVIEW .....</b>	<b>8</b>
2.1 Introduction .....	8
2.2 Biosensor .....	8
2.3 Electrochemical Biosensor.....	10
2.3.1 Glucose Biosensor.....	11
2.3.2 Non-Invasive Glucose Biosensor.....	13
2.4 Transducer Materials.....	16
2.4.1 Graphene.....	17
2.4.2 Conducting Polymers-PEDOT:PSS.....	26
2.4.3 Graphene with PEDOT:PSS as Transducer Materials.....	28
2.5 Biorecognition System .....	32
2.6 Electrochemical Characterization.....	39
2.6.1 Electrode System in an Electrochemical Cell.....	39
2.6.2 Cyclic Voltammetry as an Electroanalytical Tool.....	40
2.6.2.1 Electrochemical Reversibility.....	43
2.6.2.2 Mass Transport Properties .....	44
2.7 Machine Learning .....	46
2.7.1 Support Vector Machine.....	47
2.7.1.1 Kernel Functions.....	49
2.7.1.2 Hyperparameters Tuning.....	52



2.7.2 SVM Applications on Cyclic Voltammetry Data .....	53
2.8 Chapter Summary .....	55
<b>CHAPTER THREE: MATERIALS AND METHODOLOGY.....</b>	<b>56</b>
3.1 Introduction .....	56
3.2 Chemicals and Reagents .....	56
3.2.1 Glucose Oxidase Solution.....	57
3.2.2 Phosphate Buffered Saline Solution .....	57
3.2.3 Potassium Ferricyanide Solution.....	57
3.2.4 Graphene Oxide-Conductive Polymer Composites .....	57
3.3 Instruments.....	58
3.4 Methodology .....	59
3.4.1 Activation of Screen-printed Carbon Electrode.....	59
3.4.2 Electrochemical Reduction of GO-PEDOT:PSS.....	60
3.4.3 Immobilisation of GOx enzyme.....	61
3.4.4 Working Electrode Modification.....	62
3.4.5 Fourier Transform Infrared Spectroscopy	
Characterization.....	66
3.4.6 Electrochemical Characterization of Transducer	
Materials .....	66
3.4.6.1 Electrochemical Reversibility.....	66
3.4.6.2 Heterogeneous Electrons Transfer Rate Constant ( $k^0$ ) ....	67
3.4.6.3 Mass Transport Properties .....	67
3.4.6.4 Effective Surface Area ( $A_{\text{eff}}$ ).....	68
3.4.7 Support Vector Machine.....	69
3.4.7.1 Pre-processing Data.....	69
3.4.7.2 SVM Modelling .....	70
3.4.7.3 Variable Interaction .....	71
3.5 Chapter Summary .....	71
<b>CHAPTER FOUR: RESULTS AND DISCUSSION .....</b>	<b>72</b>
4.1 Introduction .....	72
4.2 Fabrication of rGO-PEDOT:PSS-modified SPCE.....	73
4.2.1 Activation of SPCE.....	73
4.2.2 Reduction of rGO-PEDOT:PSS-modified SPCE.....	74
4.2.3 FTIR Analysis of rGO-PEDOT:PSS-modified SPCE .....	77
4.3 Cyclic Voltammetry Analysis of rGO-PEDOT:PSS-modified	
SPCE.....	80
4.3.1 Electrochemical Reversibility of rGO-PEDOT:PSS-	
modified SPCE .....	80
4.3.2 Heterogeneous Electron Transfer Rate Constant.....	86

4.3.3 <i>Mass Transport Properties of rGO-PEDOT:PSS-modified</i>	
SPCE.....	89
4.3.4 <i>Effective Surface Area</i> .....	91
4.4 Support Vector Machine Analysis.....	93
4.4.1 <i>Pre-processing Data</i> .....	93
4.4.2 <i>Support Vector Machine (SVM) Classifications</i> .....	94
4.4.3 <i>Variable Interaction</i> .....	96
4.5 Chapter Summary.....	99
<b>CHAPTER FIVE: CONCLUSION AND RECOMMENDATION</b> .....	100
5.1 Conclusion.....	100
5.2 Recommendations for Future Work.....	102
<b>REFERENCES</b> .....	104
<b>PUBLICATIONS</b> .....	115
<b>APPENDIX A</b> .....	116
<b>APPENDIX B</b> .....	117
<b>APPENDIX C</b> .....	125
<b>APPENDIX D</b> .....	129
<b>APPENDIX E</b> .....	130
<b>APPENDIX F</b> .....	133

## LIST OF TABLES

Table 2.1 Comparison of graphene properties with carbon nanotubes (CNT) and graphite in terms of surface area, thermal and electrical conductivity, and carrier mobility.	17
Table 2.2 Comparison between chemical, thermal and electrochemical reduction strategies for removal of oxygenated functional groups on GO surface.	22
Table 2.3 Comparison of electrochemical performances of enzymatic biosensor utilizing reduced graphene oxide (rGO) as transducer material for glucose detection. Abbreviations used in connection to “transducer material”: rGO: reduced graphene oxide, GOx: glucose oxidase, GCE: glassy carbon electrode, PGE: pencil graphite electrode.	25
Table 2.4 Summary of electrochemical biosensor utilizing graphene or rGO with PEDOT:PSS as transducer material. Abbreviations used: rGO: reduced graphene oxide, PEDOT:PSS: poly(3,4-ethylenedioxythiophene) polystyrene sulfonate, SPE: screen-printed electrode, SPCE: screen-printed carbon electrode, H <sub>2</sub> O <sub>2</sub> : hydrogen peroxide, NADH: nicotinamide adenine dinucleotide, Fe(CN) <sub>6</sub> <sup>3-/4-</sup> : ferri/ferrocyanide redox couple, CEA: carcinoembryonic antigen.	29
Table 2.5 Advantages and disadvantages of different immobilization strategies.	38
Table 3.1 Randles-Sevcik equations based on reversibility.	68
Table 3.2 Details on variables for SVM modelling	70
Table 4.1 The slope of E <sub>pc</sub> against log of scan rate (log $\nu$ )	85
Table 4.2 Optimal parameters and accuracy for training and testing datasets for linear, polynomial, and RBF kernel models.	95

## LIST OF FIGURES

- Figure 1.1 Schematic illustration of present study. The fabrication parameters were varied to generate four different fabrication methods of rGO-PEDOT:PSS-modified SPCE. The modified SPCEs were subjected to cyclic voltammetry in potassium ferricyanide and the data obtained were used for electrochemical and SVM analyses. 4
- Figure 2.1 Components of a biosensor consisting of a bioreceptor for detection of a specific analyte, a transducer for converting biorecognition reaction into electrical signal and a signal processing system for signal processing and display. 9
- Figure 2.2 Reaction mechanism for the three generations of amperometric glucose biosensor based on (A) oxygen cofactor, (B) artificial redox mediators, or (C) direct electron transfer between GOx and the electrode. S = substrate, P = product. (Wang, 2008). 12
- Figure 2.3 Examples of non-invasive glucose monitoring technologies employing optical [(a) CoG, (b) D-base], transdermal [(c) GlucoWatch, (d) SugarBeat] and electrochemical [(e) Saliva Glucose Biosensor] techniques. 16
- Figure 2.4 Chemical and 3D structure of graphite, graphene, graphene oxide, and reduced graphene oxide. Adapted from Kiew, Kiew, Lee, Imae, & Chung (2016) and Bai, Muthoosamy, Manickam, & Hilal-Alnaqbi (2019). 19
- Figure 2.5 (a) The schematic figure and (b) the proposed reduction mechanism of the chemical reduction of GO using hydrazine hydrate based on Stankovich et al. (2007). 20
- Figure 2.6 Synthesis of reduced graphene oxide using oxidation-exfoliation-reduction method. Graphite as the starting material is oxidized and exfoliated to form graphene oxide. Subsequent reduction yields reduced graphene oxide (rGO). 23
- Figure 2.7 Structure of a PEDOT: PSS complex. PEDOT chain (blue) are attached to a long chain of PSS (grey) through ionic bonding (Sanchez-Sanchez, del Agua, Malliaras, & Mecerreyes, 2019). 27

- Figure 2.8 (a) 3D structure of GOx consists of FAD cofactor (yellow), carbohydrate polymer and bound ligands (green) and the (b) chemical structure of FAD, BMA, MAN and NAG. Image from the RCSB PDB (rcsb.org) of PDB ID 1CF3 (Wohlfahrt et al.,1999). 33
- Figure 2.9 Schematic illustration for immobilisation of GOx enzyme using physical adsorption on rGO-chitosan composite from previous study by Rabti, Argoubi, & Raouafi (2016). 35
- Figure 2.10 Immobilisation of GOx enzyme through covalent binding with GO.(a) The covalent bonding is formed with the presence of 1-ethyl-3-(3-dimethylamino-propyl) carbodiimide hydrochloride (EDC) and N-hydroxyl succinimide (NHS) and (b) through mixing of GOx with GO, forming GO-GOx conjugate. Redrawn from Liu, Yu, Zeng, Miao, & Dai (2010) and Alwarappan, Liu, Kumar and Li (2010). 36
- Figure 2.11 (a) 2D (left) and 3D (right) structure of glutaraldehyde comprised of 5 carbon and aldehyde functions at C-1 and C-5.(b) Glutaraldehyde cross-linking through amine groups of GOx enzyme. 37
- Figure 2.12 A typical cyclic voltammogram using potassium ferricyanide,  $K_3[Fe(CN)_6]$  as redox active analyte. The scan starts at V1 and sweeps forward to more negative potentials to reduce  $Fe(CN)_6^{3-}$  to  $Fe(CN)_6^{4-}$  and reverse to V2 to oxidized  $Fe(CN)_6^{4-}$  to  $Fe(CN)_6^{3-}$ . The anodic and cathodic peak currents ( $I_{pa}$ ,  $I_{pc}$ ) and peak potentials ( $E_{pa}$ ,  $E_{pc}$ ) are important characteristics of CV. 41
- Figure 2.13 Optimal hyperplane, margin and support vectors for linearly variable data using SVM algorithm for 2-dimensional space. Two classes of data (identified with blue and green colour) is classified by finding the optimal hyperplane with maximized margin. 48
- Figure 2.14 Soft margin classification for two classes of data using (a) small  $c$  and (b) large  $c$  in which result in misclassification of data or smaller margin, respectively. 50
- Figure 2.15 Illustration on how linear, polynomial (degree 2 and 3), and radial basis function kernel classifying two groups of data (purple and green dots). The solid line indicates the decision boundary and the dashed lines indicate the margin (Hefinioanrhy, 2019) . 52

- Figure 2.16  $K$ -fold cross-validation process for  $k=5$ . The data is divided into 5 subsets; 4 subsets is used for training data (blue) using hyperparameters and 1 subset is used as validation data (green) for the model constructed using the hyperparameters. The performance of the model is measured from the average accuracy of the 5 folds process. 53
- Figure 3.1 Screen-printed carbon electrodes (SPCE) with 2 mm diameter working electrode, a silver/silver chloride (Ag/AgCl) reference electrode and a carbon counter electrode. A RM 0.20 coin is pictured for size comparison. 58
- Figure 3.2 Schematic illustration showing overall methodology of this study. 59
- Figure 3.3 Fabrication process for transducer fabrication methods of A, B, C, and D. All SPCEs were activated before subsequent processes were carried out. The sequence of GOx immobilisation, the presence of glutaraldehyde as cross-linker, and reduction cycles of A,B,C and D were varied. 62
- Figure 3.4 Modification of SPCE using fabrication method A. A volume of 5  $\mu\text{L}$  of GO-PEDOT:PSS composite was drop-casted on the WE and was dried for 3 hours. Next, 3  $\mu\text{L}$  of GOx enzyme solution was immobilized and allowed to be adsorbed on the GO-PEDOT:PSS/SPCE at ambient temperature for 24 hours before electrochemical reduction process was carried out via CV in 0.01 M PBS, pH 5 solution. 63
- Figure 3.5 Modification of SPCE using fabrication method B. A volume of 5  $\mu\text{L}$  of GO-PEDOT:PSS composite was drop-casted on the WE and was dried for 3 hours. Next, electrochemical reduction process was carried out via CV in 0.01 M PBS, pH 5 solution. For immobilisation of GOx enzyme, 3  $\mu\text{L}$  of GOx enzyme solution was drop-casted on rGO-PEDOT:PSS/SPCE and allowed to be adsorbed on the GO-PEDOT:PSS/SPCE at ambient temperature for 24 hours before used. 64
- Figure 3.6 Modification of SPCE using fabrication method C. A volume of 5  $\mu\text{L}$  of GO-PEDOT:PSS composite was drop-casted on the WE and was dried for 3 hours. Next, electrochemical reduction process was carried out via CV in 0.01 M PBS, pH 5 solution. For immobilisation of GOx enzyme, 4.2  $\mu\text{L}$  of GOx-glutaraldehyde mixture (GOx mixed with 2% glutaraldehyde in the ratio 5:2) was drop-casted on rGO-PEDOT:PSS/SPCE followed by incubation at ambient temperature for 24 hours before used (Wisitsoraat et al., 2013). 64

- Figure 3.7 Modification of SPCE using fabrication method D. A volume of 50  $\mu\text{L}$  of GO-PEDOT:PSS composite was mixed with 30  $\mu\text{L}$  of GOx enzyme to form covalent bonding. A volume of 8  $\mu\text{L}$  of GOx-GO-PEDOT:PSS solution was drop-casted on the WE and allowed to dry at ambient temperature for 24 hours. Next, electrochemical reduction process was carried out via CV in 0.01 M PBS, pH 5 solution (Abd-Wahab et al., 2019). 65
- Figure 3.8 Experimental setup for cyclic voltammetry (CV) showing a SPCE in an electrochemical cell partially filled with either  $\text{H}_2\text{SO}_4$ (activation), PBS(reduction) or  $\text{K}_3[\text{Fe}(\text{CN})_6]$  (CV characterization) solution connected to a potentiostat and a laptop. 65
- Figure 4.1 Representative cyclic voltammogram for activation of bare SPCE in 0.1 N  $\text{H}_2\text{SO}_4$ . The potential was scanned between 2.5 V and -2.5 V at a scan rate of 100 mV/s. The inset is the CV result from the SPCE manufacturer's manual (Screen-printed, 2019). 73
- Figure 4.2 The rGO-PEDOT:PSS layer peeled off during reduction process. 74
- Figure 4.3 Electrochemical reduction of rGO-PEDOT:PSS-modified SPCEs for fabrication methods (a) A, (b) B, (c) C, and (d) D. The measurements were taken via CV in 0.01 M PBS, pH 5 at a scan rate of 50 mV/s (number of samples,  $n=5$ ). The first reduction cycle (black) of fabrication method A, B, and C show different reduction potentials whereas fabrication method D shows gradual increase of reduction current from initial potential (0 V). 76
- Figure 4.4 FTIR spectra of rGO-PEDOT:PSS-modified SPCE for fabrication method (a) A (separate immobilization of GOx, immobilization before reduction) (b) B (without glutaraldehyde, immobilization after reduction), (c) C (with glutaraldehyde, immobilization after reduction), and (d) D (combined GOx together with rGO-PEDOT:PSS). 79
- Figure 4.5 Peak-to-peak potential separation ( $\Delta E_p$ ) data from CV in 0.1 M  $\text{K}_3[\text{Fe}(\text{CN})_6]$  at scan rate of 100 mV/s of rGO-PEDOT:PSS-modified SPCEs grouped according to reduction cycles in comparison with bare SPCE (blue line).(Error bar: standard deviation. Number of samples,  $n=5$ ). (b) Standard deviation values according to the number of reduction cycles. 81
- Figure 4.6 Cyclic voltammogram of bare SPCE in 0.1 M  $\text{K}_3[\text{Fe}(\text{CN})_6]$  at scan rate of 25, 50, 100, 150 and 200 mV/s. The inset is the linear plot of cathodic peak potential,  $E_{pc}$  against log scan rate ( $\log \nu$ ). 82

- Figure 4.7 Cyclic voltammogram of rGO-PEDOT:PSS-modified SPCEs for fabrication method (a) A, (b) B, (c) C, and (d) D for 5 reduction cycles. The measurements were taken in 0.1 M  $K_3[Fe(CN)_6]$  at scan rate of 25, 50, 100, 150 and 200 mV/s. (Number of samples, n=5). 83
- Figure 4.8 Cyclic voltammogram of rGO-PEDOT:PSS-modified SPCEs for fabrication method (a) A, (b) B, (c) C, and (d) D for 15 reduction cycles. The measurements were taken in 0.1 M  $K_3[Fe(CN)_6]$  at scan rate of 25, 50, 100, 150 and 200 mV/s. (Number of samples, n=5). 83
- Figure 4.9 Cyclic voltammogram of rGO-PEDOT:PSS-modified SPCEs for fabrication method (a) A, (b) B, (c) C, and (d) D for 30 reduction cycles. The measurements were taken in 0.1 M  $K_3[Fe(CN)_6]$  at scan rate of 25, 50, 100, 150 and 200 mV/s. (Number of samples, n=5). 84
- Figure 4.10  $E_{pc}$  against log of scan rate ( $\log \nu$ ) for fabrication methods (a) A, (b) B, (c) C, and (d) D. (Number of samples, n=5). 85
- Figure 4.11 (a) The heterogeneous electron transfer rate constant ( $k^0$ ) of bare (blue line) and rGO-PEDOT:PSS-modified SPCEs for all fabrication methods grouped according to 5, 15 and 30 reduction cycles. (Error bar : standard deviation. Number of samples, n=5). (b) Standard deviation values according to the number of reduction cycles. 87
- Figure 4.12 Anodic and cathodic peak currents versus scan rate plots of rGO-PEDOT:PSS-modified SPCEs of fabrication methods of (a) A, (b) B, (c) C, and (d) D showing linearity for all fabrication methods. 90
- Figure 4.13 Anodic and cathodic peak currents versus root-squared scan rate plots of rGO-PEDOT:PSS-modified SPCEs of fabrication methods of (a) A, (b) B, (c) C, and (d) D showing linearity for all fabrication methods. 90
- Figure 4.14(a) The  $A_{eff}$  of bare (blue line) and rGO-PEDOT:PSS-modified SPCEs for fabrication method A, B, C, and D grouped according to 5, 15 and 30 reduction cycles. All fabrication methods demonstrating improved electrochemically active area in comparison with bare SPCE (Error bar: standard deviation. Number of samples, n=5).(b) Standard deviation values according to the number of reduction cycles. 92



Figure 4.15 The first 10 rows of data (a) before and (b) after pre-processing was done. The numerical variables ( $I_{pc}$ ,  $\Delta E_p$ , Cycles, and Scan rate) were normalized while categorical variables (Gluta and GOx) were transformed into binary numerical data. The data were also randomized to avoid any bias.

94

Figure 4.16 The interaction strength of input variables : Scan rate,  $I_{pc}$ , GOx, Gluta, and Cycles with output variables :(a)  $\Delta E_p$  and (b)  $I_{pc}$  based on fabrication methods. Overall, there is a strong interaction between Cycles with  $\Delta E_p$  for all fabrication methods. On the other hand, Scan rate showed strongest interaction with  $I_{pc}$  for fabrication method A and D while GOx and Gluta showed the strongest interaction with  $I_{pc}$  for fabrication method B and C, respectively.

98

## LIST OF ABBREVIATIONS

CE	Counter electrode
CPs	Conductive polymers
CV	Cyclic voltammetry
GO	Graphene oxide
GOx	Glucose oxidase
PEDOT:PSS	Poly(3,4-ethylenedioxythiophene):poly(styrene sulfonate)
RBF	Radial basis function
RE	Reference electrode
rGO	Reduced graphene oxide
SPCE	Screen-printed carbon electrode
SVM	Support vector machine
WE	Working electrode

## LIST OF SYMBOLS

$A_{\text{eff}}$	Effective surface area of the electrode ( $\text{cm}^2$ )
$C$	Solution concentration (mole/L)
$c$	Cost hyperparameter
$E_p$	Peak potential (V)
$E_{pa}$	Anodic peak potential (V)
$E_{pc}$	Cathodic peak potential (V)
$D$	Diffusion coefficient ( $\text{cm}^2/\text{s}^2$ )
$I_p$	Peak current ( $\mu\text{A}$ )
$I_{pa}$	Anodic peak current ( $\mu\text{A}$ )
$I_{pc}$	Cathodic peak current ( $\mu\text{A}$ )
$k^o$	Heterogeneous electron transfer rate constant (cm/s)
$n$	Number of electrons transferred per mole of electroactive species
$\nu$	Scan rate of the potential (V/s)
$\Delta E_p$	Peak-to-peak potential separation (mV)
$\sigma$	Sigma hyperparameter
$\Psi$	Dimensionless parameter

# CHAPTER ONE

## INTRODUCTION

### 1.1 BACKGROUND OF THE STUDY

Electrochemical biosensors have become an attractive choice of detection service for industrial, environmental, and biomedical applications owing to its sensitivity towards analytes, low cost of construction, simple fabrication, and capability to measure a targeted analyte from a complex sample (Grieshaber, MacKenzie, Vörös & Reimhult, 2008; Hammond, Formisano, Estrela, Carrara, & Tkac, 2016). Among various types of electrochemical biosensors, glucose biosensors dominate consumer market since the concept of enzyme electrode was introduced in 1962. The market preference towards glucose biosensors is not only because of the reliability and rapid response in measuring glucose concentration from blood samples but is also due to the rise of diabetes prevalence around the world. In 2019, the global population of diabetes among adults is estimated to be 463 million, showing an increase of 62 % since the last decade (International Diabetes Federation, 2019).

Conventional glucose biosensors are considered as a gold-standard tool for diabetes monitoring. However, these biosensors involved finger-pricking which cause discomfort and pain. Thus, realization of a non-invasive glucose monitoring approach has become an ultimate goal under progress. The non-invasive approach aims for measuring glucose level in alternative bodily fluids such as tear, sweat, and saliva (Baca, Finegold, & Asher, 2007; Moyer, Wilson, Finkelshtein, Wong, & Potts, 2012; Jha, David, Saluja, Venkatesh, & Chaudhary, 2014; Gupta, Sandhu, Bansal, & Sharma, 2014; Jadoon et al., 2015;). While this approach is possible due to positive

correlation between glucose level in blood and the non-blood samples, the glucose level in the non-blood samples can be hundreds of times lower of that in blood (Makaram, Owens, & Aceros, 2014); thus, the sensing element must be sensitive enough to detect the low glucose concentration. To address the challenge to detect low glucose concentration of non-blood samples, research work on the electrode fabrication constitute the most important part where the transducer materials and enzyme immobilisation strategy greatly influenced the performance of the electrochemical biosensors.

In developing electrochemical biosensors, sensitivity and selectivity matters, hence, selection of a transducer material should aim for both a highly conductive material for sensitivity, and ability to the signal produced from the reaction between targeted analyte and biorecognition element selectively. The use of graphene with a conductive polymer, poly(3,4-ethylenedioxythiophene):poly(styrene sulfonate) (PEDOT:PSS) as the transducer material for enzymatic glucose biosensor may improve biosensors' sensitivity owing to the synergistic interaction of both materials (Zhang, Yuan, Yao, Li, & Shi, 2014). Previous studies have been performed using graphene and conductive polymer composite for the detection of various analytes such as glucose (Wisitsoraat et al., 2013; Abd-Wahab, Abdul Guthoos, & Wan Salim, 2019), ammonia (NH<sub>3</sub>) (Seekaew et al., 2014; Pasha, Khasim, Khan, & Dhananjaya, 2019), and iron (Fe) (Sundramoorthy, Premkumar, & Gunasekaran, 2016). The promising results from these studies have made the combination of graphene with PEDOT:PSS attractive as a transducer material for developing a non-invasive glucose biosensor. However, there is a need to investigate further on the composite's interaction and mechanism at the molecular level.

In this study, the rGO-PEDOT:PSS transducer layer was fabricated with four different fabrication methods in which two of the methods were adopted and modified from the previous studies by Abd Wahab et al. (2019) and Wisitsoraat et al. (2013). The fabrication parameters of GO reduction cycles (for removal of oxygen functional groups on GO surfaces), glucose oxidase (GOx) immobilisation sequence (either before or after reduction of GO), and immobilisation strategy were varied. The aim is to deduce how these fabrication parameters play their role to affect electrochemical reversibility, heterogeneous electron transfer rate constant ( $k^0$ ), mass transport properties, and effective surface area ( $A_{\text{eff}}$ ) of rGO-PEDOT:PSS-modified screen-printed carbon electrode (SPCE), all of which can be determined from cyclic voltammetry (CV).

Complex relationship between the fabrication parameters and CV measurements as input and output data may impede the progress of optimizing the fabrication parameters. Through recent advances in artificial intelligence (AI), meaningful information from biosensors data can be obtained by utilizing machine learning approaches. Support vector machine (SVM) is one of the machine learning algorithms that can be applied for data classification and regression. In present study, SVM was used to build a prediction model that can differentiate the different fabrication methods. The fabrication parameters and data obtained from CV were used as the dataset to build and test the model. Comparison between three SVM models with different characteristics known as linear, polynomial and radial-basis function (RBF) kernel was done to determine the best suited model for the biosensor's data. We also explored on how the fabrication parameters relate to the data from CV through variable interaction analysis using the best SVM model (Friedman &

Popescu, 2008; Molnar, 2018a). While SVM modelling on CV data for biosensor development has been reported previously, analysing the interaction between the input and output variables based on the model has not been done before. Therefore, this study provides new insights to advance the understanding on fabrication of rGO-PEDOT:PSS composite as transducer for biosensor development utilizing the SVM prediction model. The schematic illustration of this study is shown in Figure 1.1.

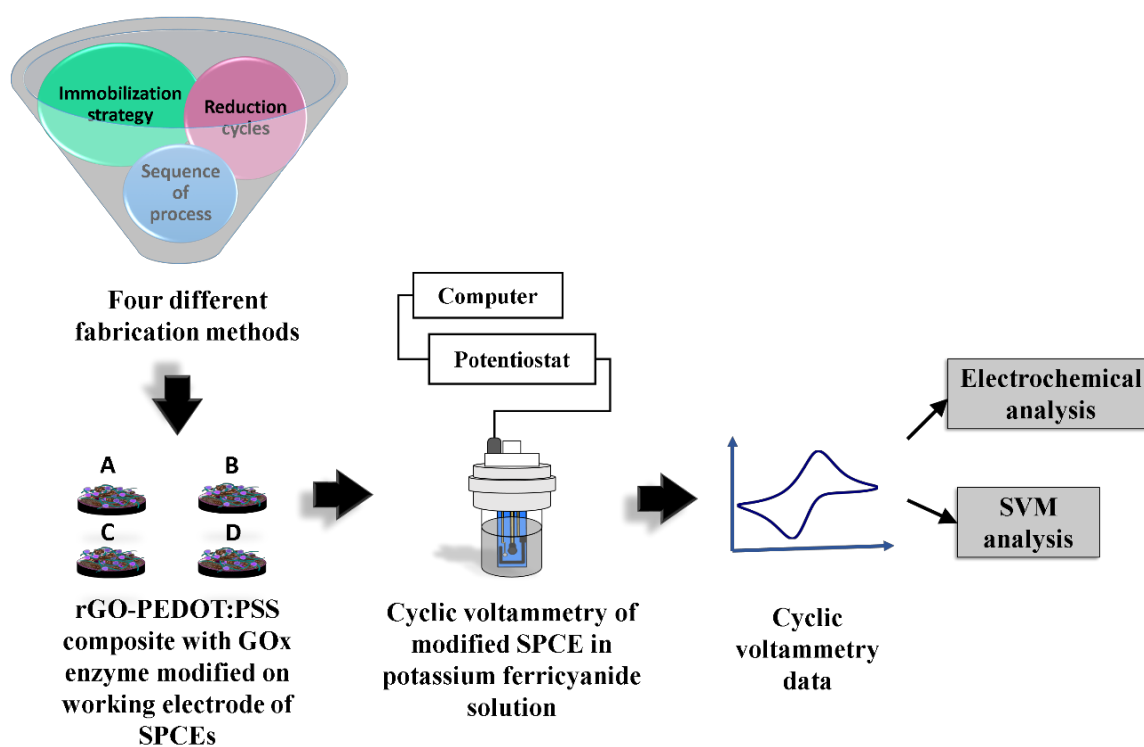


Figure 1.1 Schematic illustration of present study. The fabrication parameters were varied to generate four different fabrication methods of rGO-PEDOT:PSS-modified SPCE. The modified SPCEs were subjected to cyclic voltammetry in potassium ferricyanide and the data obtained were used for electrochemical and SVM analyses.

## 1.2 PROBLEM STATEMENT

Diabetes is a lifelong condition that requires frequent self-monitoring of blood glucose level. Conventional glucose biosensors are partially invasive where a small, sharply pointed needle is used for blood sampling. The painful finger-pricking procedure is recommended up to seven times per day, thus, discouraging many diabetes patients from managing glucose level properly. Therefore, a non-invasive device for glucose monitoring utilizing alternative bodily fluids such as saliva, sweat, and tears, is in high demand where a better diabetes control can be achieved without the pain of finger-pricking.

Employing a composite of graphene with conductive polymer, PEDOT:PSS as transducer material is expected to improve the sensitivity of glucose biosensors and enable detection of glucose in alternative bodily fluids. Fundamental research into this composite behaviour is an essential prerequisite for generating the necessary scientific understanding in developing a non-invasive glucose biosensor. In this study, the fabrication parameters were varied to observe its effect on electrochemical reversibility, heterogeneous electron transfer rate constant ( $k^0$ ), mass transport properties, and effective surface area ( $A_{\text{eff}}$ ) via cyclic voltammetry (CV). Incorporating SVM analysis for mapping the input and output data from CV may uncover relationships and interactions between data that provide deeper insights on the fabrication process.